

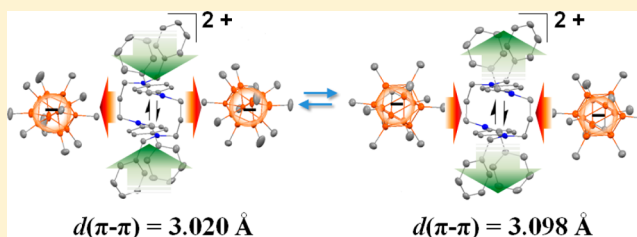
# Oxidation Products of Doubly Trimethylene-Bridged Tetrabenzyl *p*-Phenylenediamine Paracyclophane

Almaz S. Jalilov,<sup>\*,†</sup> Lu Han, Stephen F. Nelsen, and Ilia A. Guzei

Department of Chemistry, University of Wisconsin, 1101 University Avenue, Madison, Wisconsin 53711-1396, United States

**S** Supporting Information

**ABSTRACT:** We report synthesis and investigation of doubly trimethylene-bridged tetrabenzyl-*p*-phenylenediamine **1(Bz)** in its singly and doubly charged redox states. The singly oxidized monoradical cation, which is a mixed-valence (MV) system with directly interacting charge-bearing units, shows broad and solvent-sensitive intervalence bands consistent with class II compounds according to the Robin–Day classification. The doubly oxidized diradical dication of **1(Bz)** exists in the spin-paired singlet state with thermally accessible triplet state. It has similar conformations as the other dimeric *p*-phenylenediamines, such as derivatives **1(Me)** and **1(Et)**, in both the solid-state and solution phases. The successful isolation of the single-crystalline **1(Bz)**<sup>2+</sup> diradical dications with two different in nature counteranions, relatively highly coordinating SbF<sub>6</sub><sup>−</sup> and weakly coordinating carborane [undecamethylcarborane HCB<sub>11</sub>Me<sub>11</sub><sup>−</sup> (CB<sup>−</sup>)], reveals the distinct effect of the nature of counterions on the structural features of diradical dication. Cyclic voltammetry measurements of **1(Bz)** in dichloromethane reveal separation of the first and second oxidation potential by 0.12 V (2.8 kcal/mol), indicating relatively stable mixed-valence state in the dichloromethane, whereas in the acetonitrile both the first and second oxidation potentials overlap into one unresolved redox peak with minimal separation.

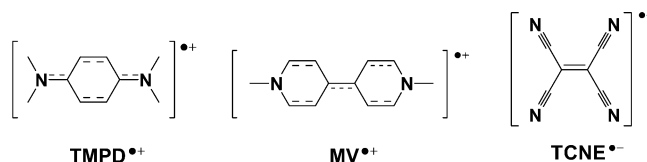


## 1. INTRODUCTION

The evolution of concept of organic radical ions has a long-standing history, which goes back at least 150 years.<sup>1</sup> Since then, radical ions have been of interest as important intermediates of chemical reactions<sup>2</sup> and crucial components for the development of new magnetic<sup>3</sup> and conducting organic and polymeric materials.<sup>4</sup> Despite considerable interest related to the open-shell organic systems (radicals), the main focus of most of the research efforts remained from the applied perspective, and details of the basic properties of the open-shell systems are still relatively scarce. One of the most well-known properties of organic radicals is their spontaneous dimerization to form  $\sigma$ -bonds (two-center, two-electron bonds).<sup>5</sup> However, many persistent radicals in which unpaired spin is delocalized over several atoms have a tendency to dimerize ( $\pi$ -dimerization) or to associate to form  $\pi$ -stacks in condensed phases.<sup>6</sup> The distances between the  $\pi$ -stacks in the solid-state structures are usually longer than the conventional covalent bonds and shorter than the sum of the van der Waals radii.<sup>7</sup> The main driving force for  $\pi$ -dimerization is known to arise from the overlap of singly occupied molecular orbitals (SOMO).<sup>8</sup> Common features of the dimers include reversibility of  $\pi$ -dimerization and lower bond strength than  $\sigma$ -dimerization. There is a large amount of literature on  $\pi$ -stacking of radical ions, extending all the way back to the 1943 hypothesis of Michaelis<sup>9</sup> that *p*-phenylenediamine radical cations (PD<sup>+</sup> derivatives) with fewer methyl groups “polymerized” at low temperature, deduced from the observed color changes. In addition, spin pairing was shown to occur in the solid state

from magnetic susceptibility measurements on crystals of less methylated compounds, whereas *N,N,N',N'*-tetramethyl-*p*-phenylenediamine<sup>+</sup> (TMPD<sup>+</sup>) neither dimerized nor spin-paired because of steric interactions between its methyl groups. It was found about 30 years later that  $\pi$ -dimers of TMPD<sup>+</sup> can be observed at much lower temperatures than that used by Michaelis<sup>10</sup> and also that the spins do pair in a low-temperature modification of TMPD<sup>+</sup>ClO<sub>4</sub><sup>−</sup> crystals.<sup>11</sup> Later, Kosower et al.<sup>12</sup> further investigated this phenomenon and discovered  $\pi$ -dimerization of viologens by studying the methyl-substituted radical cation MV<sup>+</sup> (Chart 1).

Chart 1



Several authors have reported spontaneous  $\pi$ -dimerization of another series of the persistent radical ions almost at the same time:  $\pi$ -dimerization and the question of bonding interactions between TMPD radical cations by Kimura et al.<sup>13</sup> and Nakayama and Suzuki,<sup>14</sup> 2,3-dichloro-5,6-dicyano-*p*-benzoquinone (DDQ) anion radical by Yamagishi,<sup>15</sup> and tetracyanoqui-

Received: August 29, 2013

Published: October 17, 2013

nodimethane (TCNQ) anion radicals by Boyd and Phillips.<sup>16</sup> On the basis of X-ray structures of the stretched cyclobutane-like dimers of tetracyanoethylene (TCNE) radical anion, Miller and co-workers<sup>17–19</sup> introduced the term exceptionally long four-center carbon–carbon bonding to describe them. Thereafter,  $\pi$ -dimers involving larger  $\pi$  systems have often been described as having multicenter long bonds. Theoretical discussions of the nature of their bonding interactions have been done by Head-Gordon and Jung,<sup>20</sup> Mota et al.,<sup>21</sup> and Tian and Kertesz.<sup>22</sup> Grampp et al.<sup>23</sup> in 2002 and Kochi and co-workers<sup>24</sup> in 2003 reported experimental details of the energetic parameters of the  $\pi$ -dimerizations of the best-known radical ions as well as neutral radicals. They observed that the enthalpy changes ( $\Delta H_D$ ) for  $\pi$ -dimerization (eq 1) are mainly in the range  $-6$  to  $-9$  kcal/mol and the entropy changes ( $\Delta S_D$ ) are in the range  $-30$  to  $-40$  eu. Relatively small binding energies ( $\Delta H_D$ ) and rather large negative entropy changes for  $\pi$ -dimers make these processes entropy-dominated:



In order to overcome an entropic factor, one can imagine that covalent linkage between the two interacting radicals or radical ions might give a better view of the energetic and binding effects in the  $\pi$ -dimers. Hünig and co-workers<sup>25</sup> carried out early attempts to covalently link pairs of methylviologen derivatives (Figure 1).

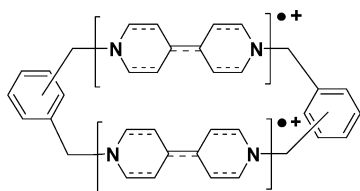
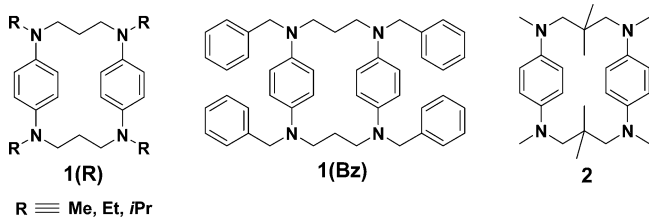


Figure 1. Doubly bridged viologen diradical dication studied by Hünig and co-workers.<sup>25</sup>

Recently we reported several works on the oxidation of “dimeric” three-carbon-bridged PD-containing [5,5]-paracyclophanes (see Chart 2).<sup>26</sup> Singly oxidized monoradical

Chart 2



cations of the paracyclophanes **1(R)** (where R = Me, Et, or *i*Pr) and **2** are mixed-valence systems with directly interacting charge bearing units.<sup>27–29</sup> According to the Robin–Day classification, these types of mixed-valence systems could be in either charge- and spin-localized (class II) or delocalized (class III) states.<sup>30</sup>

Additionally, the doubly oxidized diradical dicationic paracyclophanes, which exist almost exclusively in the  $\pi$ -dimeric spin-paired singlet states, have three isolable conformations: syn, anti, and an unsymmetrical conformation (abbreviated as uns) having one PD<sup>+</sup> ring syn and the other anti. Low-

temperature NMR studies showed that all three conformations are present in detectable amounts near  $-60$  °C (see Figure 2).<sup>27,29</sup> Unexpectedly, the methyl- and ethyl-substituted

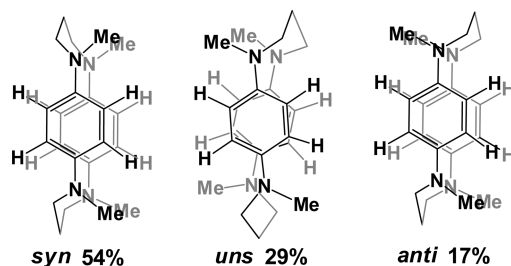


Figure 2. Relative distribution of three conformations of **1(Me)**<sup>2+</sup> at  $-60$  °C.<sup>27</sup>

compounds showed noticeably different relative populations of these conformations, with more uns than anti for **1(Me)**<sup>2+</sup> (syn:anti:uns ratio of 54:17:29) but less uns than anti for **1(Et)**<sup>2+</sup> (syn:anti:uns ratio of 68:20:12).<sup>27</sup> On the other hand, **2**<sup>2+</sup> was present exclusively in its uns conformation.<sup>29</sup> In this work, we report the effect of the benzylic substitution **1(Bz)** on the structural and electronic states of similar class of paracyclophanes in both the singly and doubly oxidized states.

## 2. RESULTS AND DISCUSSION

**2.1. Synthesis of Paracyclophane 1(Bz).** Paracyclophane **1(Bz)** was synthesized according to the procedure shown in Figure 3 from the precursor paracyclophane **1(H)**, the

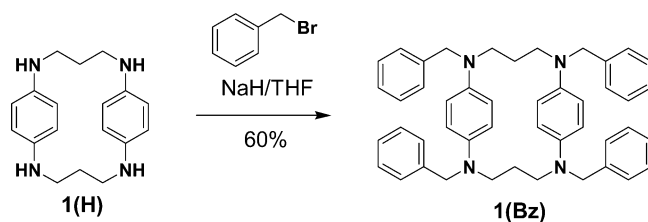
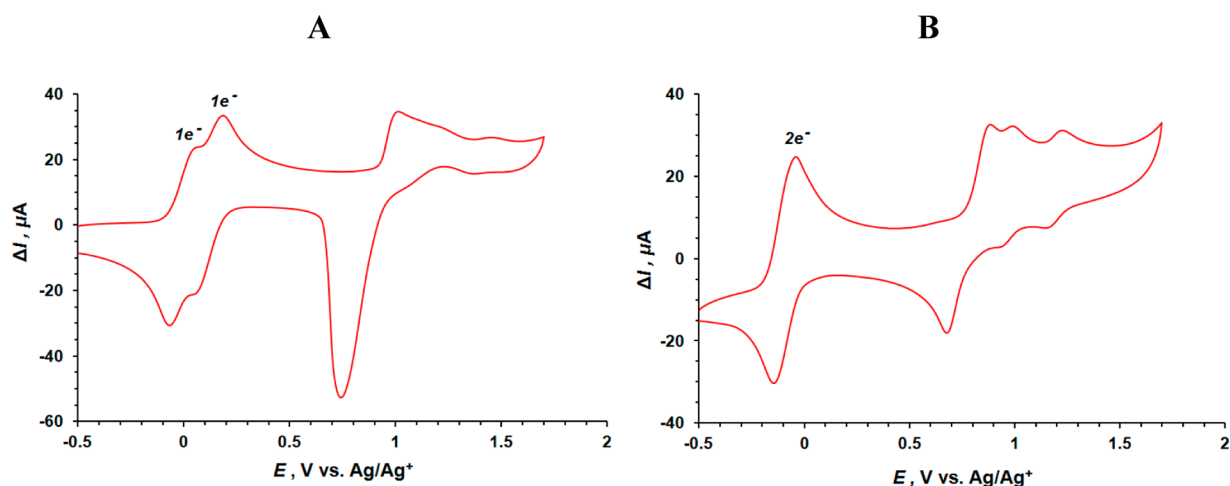


Figure 3. Synthetic route for preparation of **1(Bz)**.

synthesis of which was previously described.<sup>26</sup> **1(Bz)** was easily obtained as a yellow crystalline product by benzylation of **1(H)** with excess benzyl bromide under basic conditions in 60% yield (see Figure 3). Oxidation of apparent paracyclophanes with **1** equiv of oxidant results in the blue, relatively stable monoradical cation. By double oxidation with 2 equiv of oxidant, maroon diradical dication were obtained (see the Experimental Section for details).

**2.2. Electrochemical Measurements.** Cyclic voltammograms (CVs) for compound **1(Bz)** in two different solvents (dichloromethane, panel A, and acetonitrile, panel B) recorded at room temperature are shown in Figure 4, and the lowest oxidation potentials are summarized in Table 1. Similarly to the previously published PD-containing paracyclophanes [**1(R)**, where R = Me, Et, or *i*Pr], two regions of the oxidation potentials could be observed (Figure 4). The first region is below 0.5 V and corresponds to  $E_{1/2}(0/+1)$  and  $E_{1/2}(+1/+2)$ . The second region is above 0.5 V and corresponds to  $E_{1/2}(+2/+3)$  and  $E_{1/2}(+3/+4)$ . The unique feature of **1(Bz)** is that there is a separation of the first and second oxidation peaks ( $\Delta E^\circ$ ) in dichloromethane by 0.12 V, which corresponds to 2.8 kcal/mol. Due to the poor solubility of neutral **1(Bz)** in acetonitrile, CV



**Figure 4.** Cyclic voltammetry of (A) **1(Bz)** in 0.1 M TBAP/ $\text{CH}_2\text{Cl}_2$  solution and (B)  $\mathbf{1(Bz)^+}[\text{SbF}_6]^-$  in 0.1 M TBAP/ $\text{CH}_3\text{CN}$  solution, with Pt working electrode and scan rate  $100 \text{ mV}\cdot\text{s}^{-1}$ .

**Table 1.** Cyclic Voltammetric Data for **1(Bz)** in  $\text{CH}_2\text{Cl}_2$  and  $\text{CH}_3\text{CN}$

compd and solvent	$E_{1/2}(0/+1)^a$	$E_{1/2}(+1/+2)^a$	$\Delta E^\circ{}^b$	$K_{\text{comp}}$	Robin–Day class
<b>1(Bz)</b> in $\text{CH}_2\text{Cl}_2$	-0.01 (0.12)	0.12 (0.12)	0.13	157	II/III
<b>1(Bz)</b> in $\text{CH}_3\text{CN}$	-0.09 (0.09)	-0.09 (0.09)	$\sim 0.00$	$\sim 3^c$	II

<sup>a</sup>Potentials are given in volts vs  $\text{Ag}/\text{Ag}^+$  in the presence of supporting electrolyte 0.1 M TBAP (scan rate =  $100 \text{ mV}/\text{s}$ ). The number in parentheses is  $E^{\text{ox}} - E^{\text{red}}$ . <sup>b</sup> $\Delta E^\circ = E_1^\circ - E_2^\circ$ . <sup>c</sup>Number taken according to reported simulation data for **1(R)**.<sup>26</sup>

data of the more soluble  $\mathbf{1(Bz)^+}[\text{SbF}_6]^-$  salt were recorded. The first two oxidation peaks are overlapped into one unresolved oxidation peak (Figure 4B) and could not be distinguished, indicating that in acetonitrile the second electron is only slightly harder to remove than the first. Therefore, the relatively high degree of disproportionation for the monoradical cation of **1(Bz)** to the neutral and the diradical dication of **1(Bz)** could take place in acetonitrile, in comparison to dichloromethane. The second region of oxidation peaks, where the third and fourth oxidation waves can be observed, are irreversible in both solvents and less informative due to absorption of the less soluble polycations in organic solvents; see Figure 4.

The comproportionation equilibrium constants,  $K_{\text{comp}}$ , for **1(Bz)** in two different solvents at 298 K were determined by eq 2, where  $\Delta E^\circ$  is the difference in oxidation potentials for the first and second oxidation processes.

$$K_{\text{comp}} = \frac{[\mathbf{1(Bz)^{\bullet-}}]^2 / [\mathbf{1(Bz)^{2+}}][\mathbf{1(Bz)^{\circ}}]}{=} = \exp[\Delta E^\circ(F/RT)] \quad (2)$$

The magnitude of  $K_{\text{comp}}$  is related to electronic couplings between the charge-carrying units of the organic mixed-valence compounds.<sup>31</sup> Generally, the compounds having values of  $K_{\text{comp}}$  varying from several orders of magnitudes ( $>10^5$ ), considered as strongly coupled class III systems according to the Robin–Day classifications of mixed valency.<sup>32</sup> The comproportionation equilibrium constants for **1(Bz)** are  $K_{\text{comp}} = 157$  and  $\sim 3$  in dichloromethane and acetonitrile, respectively, suggesting a weak solvent-dependent electronic coupling between the two charge-bearing PD units to form the class II mixed-valence state in acetonitrile and stronger electronic coupling with possible formation of the class III (or borderline between class II and III states, that is, class II/III)<sup>33</sup> mixed-valence state in dichloromethane (schematically shown in Figure 5). Using Mulliken–Hush analysis for the estimation of electronic interactions, Rosokha and Kochi<sup>34</sup> showed that free TMPD radical cations forms a class II self-exchange mixed-valence state with its neutral counterpart. Solvent-sensitive electronic couplings for various dinitroaromatic radical anions are also reported in the literature.<sup>35</sup> Previously we have observed both localized (class II) and delocalized (class III) mixed-valence systems of various alkyl-substituted and bridge-modified paracyclophane radical cations.<sup>26–29</sup>

Furthermore, according to Evans and co-workers,<sup>36</sup> the reason for the reduced values of  $\Delta E^\circ$ , known as potential compression, is either through a significant geometric change of

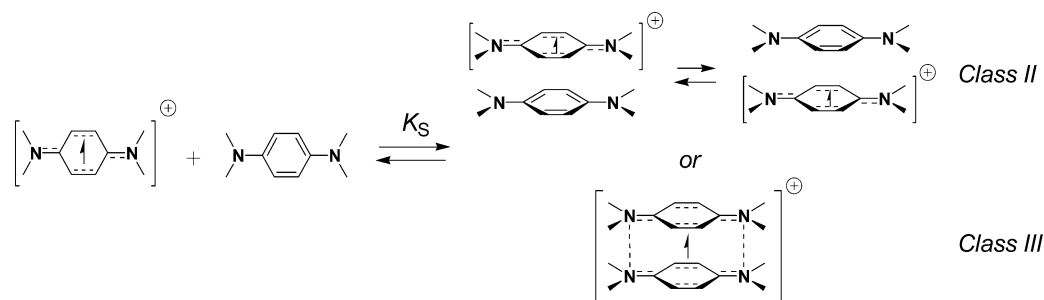


**Figure 5.** Schematic representation of two different mixed-valence states in dimeric TMPD radical cations.

redox species upon the first and second oxidation processes or through ion pairing between oxidized radical cations and anions of the supporting electrolytes. For **1(Bz)** with the geometrically flexible trimethylene bridge, we have shown that there is a minor geometric change between the singly and doubly oxidized species, **1(R)<sup>+</sup>** and **1(R)<sup>2+</sup>**, respectively.<sup>29</sup> Therefore, we assume that specific ion-pairing interactions, particularly radical cation–solvent interactions (vide infra) could be the major contribution to the potential compression of **1(Bz)**, resulting in the localized nature of mixed-valence species in the more polar acetonitrile.

**2.3. Oxidation Products of 1(Bz).** **2.3.1. Radical Cation of 1(Bz).** Oxidation of **1(Bz)** in three different solvents with 1 equiv of the oxidant  $\text{NO}^+\text{SbF}_6^-$  results in the optical spectra of oxidation products of **1(Bz)** shown in Figure 6. As for the

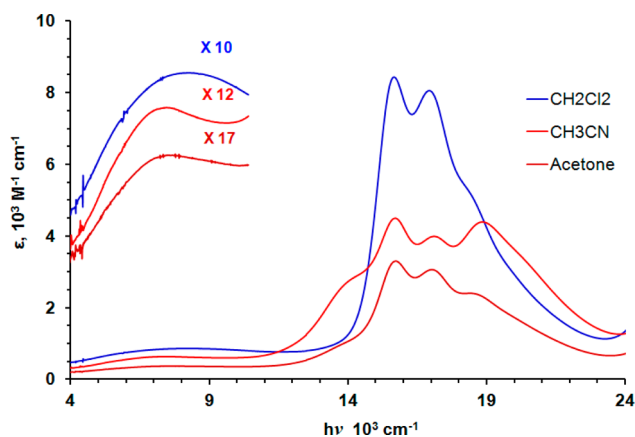


**Figure 6.** Visible–near-IR spectra of **1(Bz)<sup>+</sup>[SbF<sub>6</sub>]<sup>-</sup>** in various solvents. We note the broadening of the spectrum in acetonitrile and in acetone due to overlapping with the optical spectra of doubly oxidized product.

methyl and ethyl derivatives **1(Me)** and **1(Et)**, respectively, the monoradical cation of **1(Bz)** has two lowest-energy absorption bands in the visible and the near-IR region. Particularly, the monocationic and dicationic oxidation states of **1(Bz)** closely resemble the optical spectra of **1(Et)<sup>+</sup>** and **1(Et)<sup>2+</sup>**, respectively (see Figures 6 and 7).<sup>26,27</sup> The strongest electronic absorption of **1(Bz)<sup>+</sup>** at  $15\,700\text{ cm}^{-1}$  with resolved vibrational structures

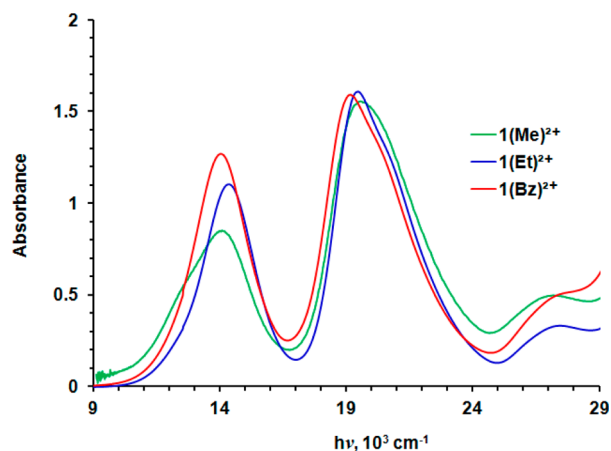


**Figure 7.** Comparison of room-temperature optical spectra of **1(Me)<sup>2+</sup>**, **1(Et)<sup>2+</sup>**, and **1(Bz)<sup>2+</sup>**. Absorptions are scaled arbitrarily.

corresponds to the electronic transition from the highest doubly occupied molecular orbital to the singly occupied molecular orbital (HOMO to SOMO) within the singly oxidized PD unit. The second strongest energy transition in the near-IR region is relatively weak and structureless. These are typical mixed-valence transition bands corresponding to the single electron transfer between oxidized and neutral PD units.<sup>26,29</sup> For **1(Bz)<sup>+</sup>**, the maxima and shape of the mixed-valence band are strongly dependent on the nature of the solvent environment, as shown in Figure 6.

As suggested in the previous section, we assign mixed-valence bands in dichloromethane as borderline class II/III (delocalized) and in acetonitrile as class II (localized) charge-transfer bands.

**2.3.2. Diradical Dication of 1(Bz).** Maroon diradical dication **1(Bz)<sup>2+</sup>** was formed by oxidizing **1(Bz)** with 2 equiv of oxidant in organic media. Vis/NIR spectrum of **1(Bz)<sup>2+</sup>** in acetonitrile shows two distinct absorbances at  $13\,600\text{ cm}^{-1}$  and at  $19\,100\text{ cm}^{-1}$ .

As shown in Figure 7, the optical spectrum of **1(Bz)<sup>2+</sup>** in acetonitrile clearly resembles that of **1(Et)<sup>2+</sup>** with a slight red shift in both of the absorbance maxima. **1(Me)<sup>2+</sup>** has a considerably higher percentage of uns conformations, which absorb at a lower energy than the syn and anti conformations,<sup>27</sup> than **1(Et)<sup>2+</sup>**. Consistent with this expectation, the optical spectrum of **1(Me)<sup>2+</sup>** shows a clear bulge (around  $12\,500\text{ cm}^{-1}$ ) on the low-energy side of the first absorption band (see Figure 7), which we attributed to the contribution of its uns conformation to the spectrum. The lack of this bulge for **1(Bz)<sup>2+</sup>** suggests that **1(Bz)<sup>2+</sup>** also has a much smaller percentage of uns conformations than **1(Me)<sup>2+</sup>**.

According to the results for **1(Me)<sup>2+</sup>** and **1(Et)<sup>2+</sup>**,<sup>27</sup> we assign two of the lowest electronic absorptions to the bonding and antibonding combination of PD<sup>+</sup> singly occupied molecular orbitals (SOMOs), that is, HOMO to LOMO (lowest unoccupied molecular orbital) and HOMO – 1 to LUMO transitions of the formed dimeric (PD<sup>+</sup>)<sub>2</sub> unit, respectively (as schematically shown in Figures 8 and 9).

Variable-temperature <sup>1</sup>H NMR spectra of **1(Bz)<sup>2+</sup>·2[SbF<sub>6</sub>]<sup>-</sup>** in CD<sub>3</sub>CN/CD<sub>3</sub>OD (2:1 mixture by volume) reveals broad peaks for the protons of PD<sup>+</sup> units at room temperature, which sharpen up considerably upon lowering the temperature to  $-50\text{ }^\circ\text{C}$  (see Figure 10). As we have shown previously, these types of diradical dications have a singlet ground state with thermally accessible triplet states.<sup>26</sup> Unlike <sup>1</sup>H NMR spectra of **1(Me)<sup>2+</sup>** and **1(Et)<sup>2+</sup>**, the spectrum of **1(Bz)<sup>2+</sup>** was uninformative due to poorer solubility at low temperatures and broader peaks as shown in Figure 10. However, we could still clearly observe aromatic protons around 6 ppm, which correspond to the syn and anti conformations of the diradical dications.

It might be conceivable that relative distributions of the conformational isomers (syn, anti, and uns) differ in solution and solid phases. In order to get further insight into the nature of conformational distribution in the solid state, we recorded diffusion reflectance spectra of the solid diradical dication salt **1(Bz)<sup>2+</sup>·2[SbF<sub>6</sub>]<sup>-</sup>**. Figure 11 shows comparison of the spectrum in acetonitrile (at room temperature) with that of the solid salt **1(Bz)<sup>2+</sup>·2[SbF<sub>6</sub>]<sup>-</sup>**, which shows similar band shapes in both media. It is clear from the lowest energy absorption bands of the solid-state spectrum that, as in the solution, it mainly consists of syn and anti conformations in solid phase.



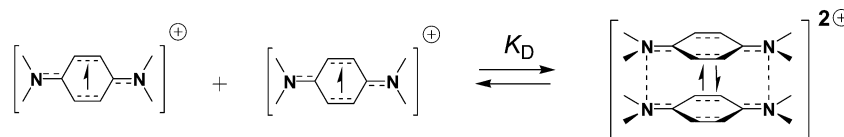


Figure 8. Self-dimerization of TMPD radical cations to form diamagnetic diradical dication.

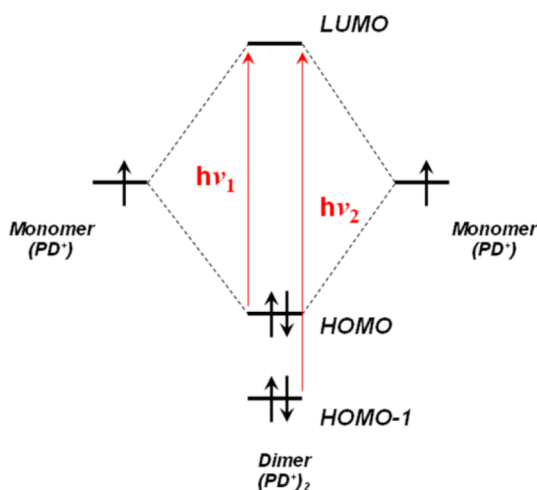


Figure 9. Simplified molecular orbital (MO) energy diagram of PD dimer dication.

**X-ray Crystallographic Data of Diradical Dications.** Slow diffusion of hexane into a maroon solution of  $1(\text{Bz})^{2+} \cdot 2[\text{SbF}_6]^-$  in acetone at  $-30^\circ\text{C}$  gives black single crystals suitable for X-ray crystallography. The unit cell contains one dication, two anions, and four molecules of solvent acetone, to form the general structure of crystal packing as  $[(\text{C}_{46}\text{H}_{48}\text{N}_4^{2+}) \cdot (\text{SbF}_6^-)_2(\text{C}_3\text{H}_6\text{O})_4]_n$ . The  $\pi$ -dimeric diradical dication resides on a crystallographic inversion center, thus the asymmetric unit (symmetry-independent part of the lattice) contains half of the dication, one anion, and two molecules of solvent acetone, as shown in Figure 12. The  $\pi$ -dimeric diradical dication is in the

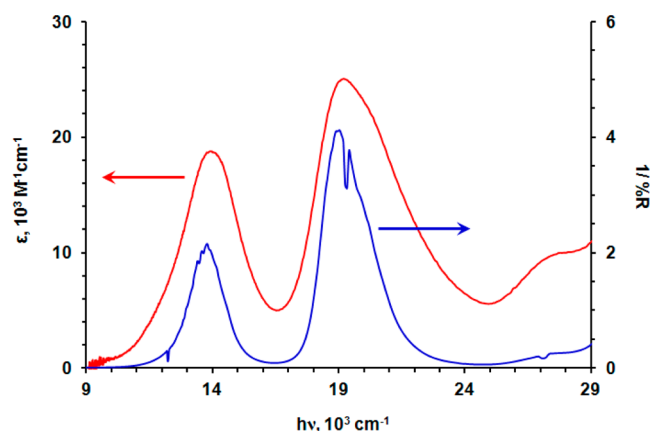


Figure 11. Visible–near-IR spectrum of  $1(\text{Bz})^{2+} \cdot 2[\text{SbF}_6]^-$  in acetonitrile (red) and reflectance spectra of solid  $1(\text{Bz})^{2+} \cdot 2[\text{SbF}_6]^-$  (blue). The reflectance spectrum of solid  $1(\text{Bz})^{2+} \cdot 2[\text{SbF}_6]^-$  has two strong lowest-energy absorptions at  $13\,600$  and  $19\,100\text{ cm}^{-1}$ , which is similar to the optical spectrum in solution.

anti conformation, structurally similar to the methyl and ethyl derivatives. The distance between the two nitrogen atoms in contact with adjacent PD units ( $\text{N}-\text{N}$  as shown in Figure 12) is  $2.9480(13)\text{ \AA}$ , shorter than the sum of the out-of plane van der Waals radii of the two nitrogen atoms ( $3.10\text{ \AA}$ ). Additionally, each  $\pi$ -stacked dimeric unit is stabilized by two counterions ( $\text{SbF}_6^-$ ) via the  $\text{H-bond C15}-\text{H}\cdots\text{F3}$ , which has a distance of  $2.579\text{ \AA}$ , and also by two close solvent molecules through  $\text{H-bond C10}-\text{H}\cdots\text{O2}$ , which has a distance of  $2.220\text{ \AA}$  (Figure 12).

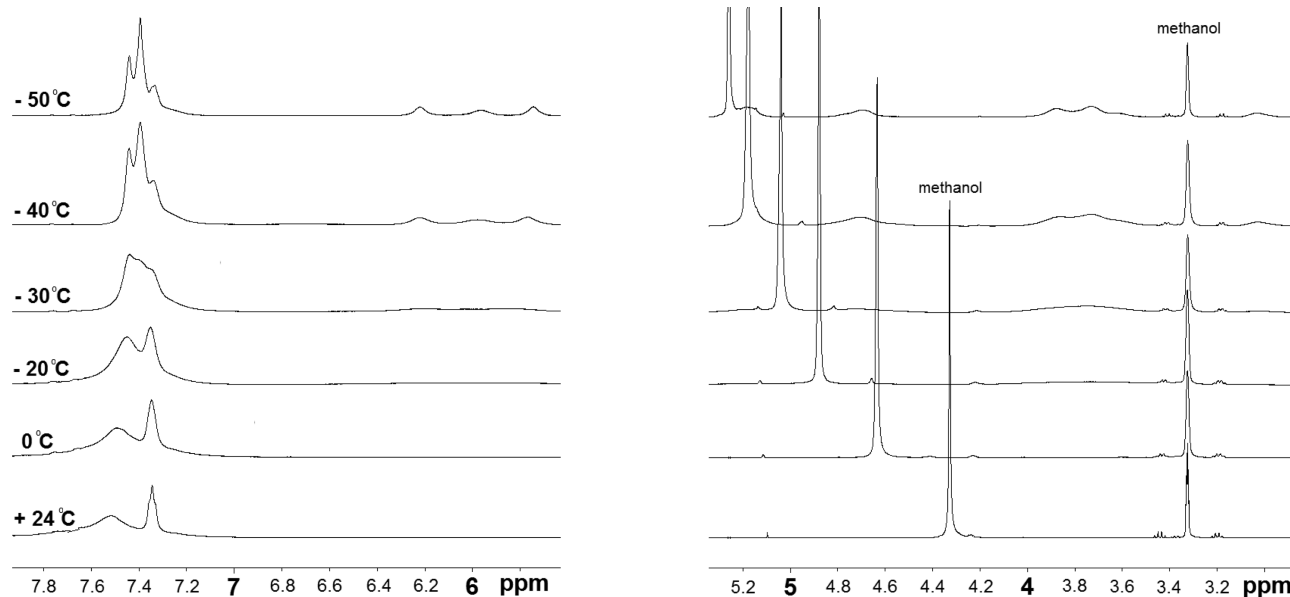
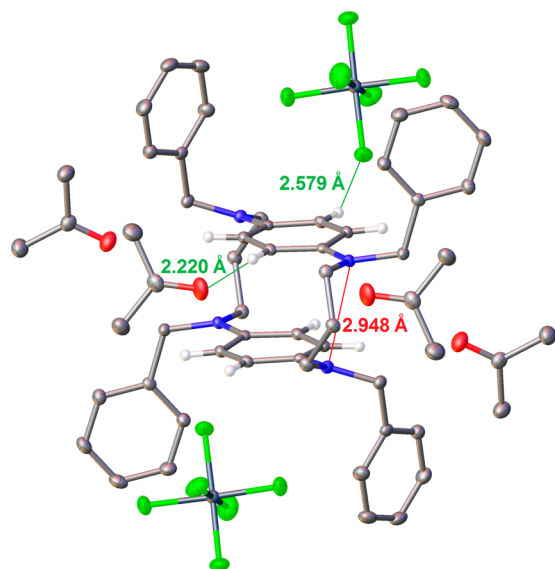
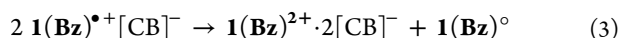


Figure 10. Variable-temperature  $^1\text{H}$  NMR spectrum of  $1(\text{Bz})^{2+} \cdot 2[\text{SbF}_6]^-$  in  $\text{CD}_3\text{CN}/\text{CD}_3\text{OD}$  (2:1 mixture by volume). A strong temperature-dependent singlet peak corresponds to the hydroxyl group of the solvent methanol.



**Figure 12.** X-ray structure of  $1(\text{Bz})^{2+} \cdot 2[\text{SbF}_6]^- \cdot 4\text{Me}_2\text{C}=\text{O}$ . Hydrogen atoms are omitted for clarity except for hydrogen atoms of the PD unit. Only the symmetry-independent atoms are labeled. Molecular diagrams are drawn with 50% probability ellipsoids.

Upon slow diffusion of hexane at  $-30\text{ }^\circ\text{C}$  to the blue dichloromethane solution of monoradical cationic salt of  $1(\text{Bz})$  and weakly coordinated counterion undecamethylcarborane  $\text{HCB}_{11}\text{Me}_{11}^- (\text{CB}^-)$ , diradical dication can be isolated as a product of the disproportionation reaction (eq 3). Undecamethylcarborane ( $\text{CB}^-$ ), known as a weakly coordinating and inert anion, is used preferably for isolation of reactive cations and strong oxidants.<sup>37</sup>



The asymmetric unit contains two halves of two symmetry-independent dications [ $1(\text{Bz})^{2+}$ ], two full anions ( $\text{CB}^-$ ), and four full dichloromethane molecules. The two conformational isomers of dications reside on crystallographic inversion centers. Therefore the ratio between species is 2 dications:4 anions:8 dichloromethane solvent molecules to form a general structure of  $[(\text{C}_{46}\text{H}_{48}\text{N}_4^{2+})_2(\text{CB}^-)_4(\text{CH}_2\text{Cl}_2)_8]_n$ . One of the

dichloromethane molecules is disordered over two positions with a 75.5(6)% major component and was refined with constraints and restraints. Both of the two independent diradical dications  $1(\text{Bz})^{2+} \cdot 2[\text{CB}]^-$  are in their anti conformations. The presence of the two independent diradical dications that differ in the conformational features within the same unit cell gives us an opportunity to discuss the effect of counterion on the weak  $\pi-\pi$  dimeric interactions of two independent diradical dications within the same single crystal. The most significant features of the structural details of the two independent diradical dications of  $1(\text{Bz})^{2+} \cdot 2[\text{CB}]^-$  and  $1(\text{Bz})^{2+} \cdot 2[\text{SbF}_6]^-$  are summarized in Table 2. For clarity we will abbreviate the two independent isomeric structures of  $1(\text{Bz})^{2+} \cdot 2[\text{CB}]^-$  within the same unit cell as  $1(\text{Bz})^{2+} \cdot 2[\text{CB}]^-$  (A) and  $1(\text{Bz})^{2+} \cdot 2[\text{CB}]^-$  (B). As listed in Table 2,  $1(\text{Bz})^{2+} \cdot 2[\text{CB}]^-$  (B) has fairly similar structural details to  $1(\text{Bz})^{2+} \cdot 2[\text{SbF}_6]^-$ , but  $1(\text{Bz})^{2+} \cdot 2[\text{CB}]^-$  (A) has longer  $\pi-\pi$  distances between two  $\text{PD}^+$  units.

To compare structural details of the two independent diradical dications, we identified the shortest intermolecular distances between the diradical dications and the counteranions. By doing so, the four shortest H-bonding contacts  $\text{C}-\text{H} \cdots \text{CH}_3$  between methyl groups of the two counteranions ( $\text{CB}^-$ ) and  $\text{C}-\text{H}$  hydrogens of the  $\pi-\pi$  dimeric  $\text{PD}^+$  radical cations were identified as shown in Figure 13. For  $1(\text{Bz})^{2+} \cdot 2[\text{CB}]^-$  (A) with two symmetrical N1–N2 distances of 2.982 Å, the two shortest H-bonding contacts  $\text{C}-\text{H} \cdots \text{CH}_3$  are 2.844 and 3.050 Å. Similarly, the numbers for  $1(\text{Bz})^{2+} \cdot 2[\text{CB}]^-$  (B) are  $d(\text{N3}-\text{N4}) = 2.950\text{ } \text{Å}$  and  $d(\text{C}-\text{H} \cdots \text{CH}_3) = 2.947$  and 3.083 Å. Here one can observe that the shorter  $\pi-\pi$  interactions between  $\text{PD}^+$  units of the diradical dication  $1(\text{Bz})^{2+} \cdot 2[\text{CB}]^-$  (B) have longer intermolecular counteranion–radical cation interactions ( $\text{C}-\text{H} \cdots \text{CH}_3$ ). The opposite was observed for longer  $\pi-\pi$  interactions in the diradical dication  $1(\text{Bz})^{2+} \cdot 2[\text{CB}]^-$  (A), with shorter counteranion–radical cation interactions.

### 3. CONCLUSIONS

Changing the R group from methyl and ethyl to benzyl in the “dimeric” three-carbon-bridged  $\text{PD}^+$ -containing [5,5]-paracyclophanes significantly increases the separation of the first and second oxidation peaks in dichloromethane. The singly

**Table 2.** Comparison of  $1(\text{Bz})$  Dication X-ray Structures

	$1(\text{Bz})^{2+} \cdot 2[\text{SbF}_6]^- \cdot 4\text{Me}_2\text{C}=\text{O}$ (N26)	$1(\text{Bz})^{2+} \cdot 2[\text{CB}]^- \cdot 4\text{CH}_2\text{Cl}_2$ (A) (N27) <sup>a</sup>	$1(\text{Bz})^{2+} \cdot 2[\text{CB}]^- \cdot 4\text{CH}_2\text{Cl}_2$ (B) (N27) <sup>a</sup>
NCCC conformations	gg, gg	gg, gg	gg, gg
PD conformations	anti, anti	anti, anti	anti, anti
dication symmetry	$C_i$	$C_i$	$C_i$
$d(\text{N}-\text{N})$ (Å)	2.948	2.982	2.950
$d(\text{C}_q-\text{C}_q)^b$ (Å)	3.053	3.099	3.050
$d(\text{CH}-\text{CH})^c$ (Å)	3.106	3.161	3.111
$d(\text{CH}-\text{CH})^c$ (Å)	3.160	3.234	3.173
$d[\text{N}-\text{CH}_2(\text{br})]$ (Å)	1.469, 1.476	1.464, 1.468	1.463, 1.477
$d(\text{N}-\text{R})$ (Å)	1.468, 1.481	1.468, 1.474	1.471, 1.473
$d(\text{CH}_2-\text{R}')$ (Å)	1.516, 1.523	1.509, 1.520	1.509, 1.516
$d(\text{mean } C_6 \text{ planes})$ (Å)	2.988	3.098	3.020
PD ring displacement <sup>d</sup> (Å)	0.93	0.65	0.76
NCCC twists (deg)	-6.62, 65.69	-66.74, 65.80	-66.70, 65.74
NCCC twists (deg)	66.62, -5.69	66.74, -65.80	66.70, -65.74

<sup>a</sup>Unit cell contains two independent dications. <sup>b</sup>Distance between pairs of quaternary ring carbons. <sup>c</sup>Distance between the closest ring CH carbons.

<sup>d</sup>Measured from the perpendicular to the average  $C_6$  plane.

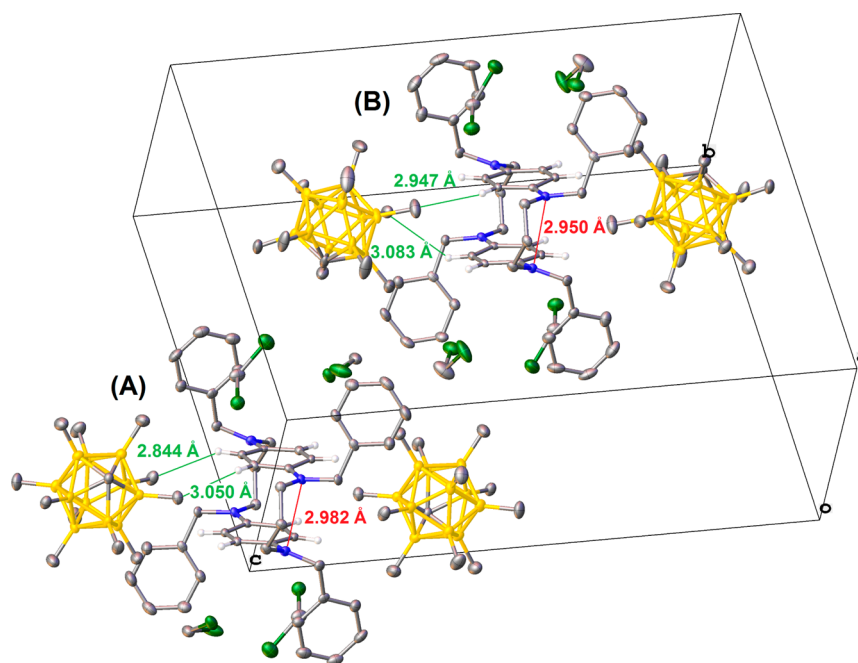


**Figure 13.** Fragment of unit cell of  $1(\text{Bz})^{2+} \cdot 2[\text{CB}]^{-} \cdot 4\text{CH}_2\text{Cl}_2$  (A) and  $1(\text{Bz})^{2+} \cdot 2[\text{CB}]^{-} \cdot 4\text{CH}_2\text{Cl}_2$  (B). Hydrogen atoms are omitted for clarity except for hydrogen atoms of the PD unit. Molecular diagrams are drawn with 50% probability ellipsoids.

oxidized monoradical cation  $1(\text{Bz})^{\cdot+}$  reveals broad and solvent-sensitive intervalence band indicative of weak electron-localized class II mixed-valence system. Furthermore, the doubly charged diradical dication  $1(\text{Bz})^{2+}$  exhibit similar conformational features as ethyl derivative  $1(\text{Et})^{2+}$  in both the solid state and solution phases. The diradical dication  $1(\text{Bz})^{2+}$  was isolated as single-crystalline ion-paired salts with two different counterions,  $\text{SbF}_6^{-}$  and a less coordinating carborane anion, undecamethylcarborane  $\text{HCB}_{11}\text{Me}_{11}^{-}$  ( $\text{CB}^{-}$ ). Luckily, the carborane anion-containing salt  $1(\text{Bz})^{2+} \cdot 2[\text{CB}]^{-}$  crystallized in two conformationally isomeric structures within the same unit cell. These conformationally isomeric structures,  $1(\text{Bz})^{2+} \cdot 2[\text{CB}]^{-}$  (A) and  $1(\text{Bz})^{2+} \cdot 2[\text{CB}]^{-}$  (B), differ in both intramolecular  $\pi$ - $\pi$  distances (PD $^+$ -PD $^+$  separations) and intermolecular diradical dication  $1(\text{Bz})^{2+}$ -counteranion  $2\text{CB}^{-}$  distances.

Together with previous studies,<sup>26–29,38</sup> this work shows that molecular interactions of the organic radical ions are clearly sensitive to the solvent and counterion environment, which is also shown by theoretical studies on the spontaneous dimerization of TMPD radical cations.<sup>39</sup> We expect that deeper understanding from the molecular perspective of the intermolecular binding nature of the open-shell organic radicals can provide the basis for future discoveries of novel organic materials.

#### 4. EXPERIMENTAL SECTION

**4.1. *N,N',N'',N'''* Tetrabenzyl-1,5,12,16-tetraaza[5,5]-paracyclophane, 1(Bz).** 1,5,12,16-Tetraaza[5,5]paracyclophane  $1(\text{H})^{26}$  (2.53 g, 8.5 mmol) was immersed in anhydrous tetrahydrofuran (THF, 40 mL). Under nitrogen, 1.68 g (70 mmol) of NaH was added to the solvent. The mixture was heated under reflux for 1 h. After that, 4.45 g (25.5 mmol) of benzyl bromide was added to the mixture. The mixture was stirred for 1 h and evaporation was conducted to get rid of extra benzyl bromide and THF. Methanol (300 mL) was added dropwise to the product that remained. The resultant solution was filtered, and the residue was washed with hexane and left to dry in air. The product was further separated by column

chromatography to give 3.4 g of yellow-white crystalline product (60% yield): UV 263 nm in  $\text{CH}_2\text{Cl}_2$ ; mp 190–194 °C;  $^1\text{H}$  NMR ( $\text{CDCl}_3$ , 300.137 MHz)  $\delta$ , ppm 7.28 (m, 4H), 7.23 (s, 4H), 6.60 (s, 8H), 4.25 (s, 8H), 3.16 (t, 8H), 1.61 (m, 4H);  $^{13}\text{C}$  NMR ( $\text{CDCl}_3$ , 300.137 MHz):  $\delta$ , ppm 141.5, 140.1, 128.6, 127.9, 127.0, 118.36, 58.3, 49.1, 21.6; HR-MS TOF MS ES+ calcd  $[\text{M} + \text{H}]^+ = 656.384$  monoisotopic, measd  $[\text{M} + \text{H}]^+ = 656.3877$  (<1 ppm).

**4.2. Oxidation Reactions.** Radical cation and diradical dication salts  $1(\text{R})^{\cdot+} \cdot [\text{X}]^{-}$  and  $1(\text{R})^{2+} \cdot 2[\text{X}]^{-}$ , were prepared by oxidation of the corresponding neutral compounds with stoichiometric (1:1 or 1:2) amounts of corresponding silver or nitrosonium salts ( $\text{Ag}^+\text{CB}^{-}$  or  $\text{NO}^+\text{SbF}_6^{-}$ , respectively) in dichloromethane, with a small amount of acetonitrile added for preparation of the dication in order to increase the solubility of the diradical dication salt. The resulting dark blue solution of radical cation or maroon solution of diradical dication salts was precipitated by use of an excess amount of hexanes. Silver undecamethylcarborane [ $\text{Ag}^+\text{CB}^{-}$ ] was prepared by an analogous method to the literature procedure from  $\text{Cs}^+$  [ $\text{HCB}_{11}\text{Me}_{11}^{-}$ ] and  $\text{AgNO}_3$ .<sup>40</sup> For the oxidation with  $\text{NO}^+\text{SbF}_6^{-}$ , it is important to bubble the resulting reaction mixture with inert gas for several minutes in order to remove the product NO gas, which forms adducts with radical cations. Single crystals of the dication diradical salt  $1(\text{Bz})^{2+} \cdot [\text{SbF}_6]^{-}$  were prepared by dissolving the diradical dication salt in acetone, and the resulting clear maroon solution was overlaid with a small amount of the mixture of acetone and diethyl ether, which was again overlaid with diethyl ether. Analogously, single-crystalline  $1(\text{Bz})^{2+} \cdot 2[\text{CB}]^{-}$  was prepared by dissolving the monoradical cation salt in dichloromethane and the resulting clear solutions were overlaid with a small amount of the mixture of dichloromethane and hexanes, which was again overlaid with hexane. The solvent mixtures were kept in a low-temperature refrigerator at  $-80$  °C for several days. Radical ions crystallize with solvent molecules that easily evaporate, making them difficult to handle and to weigh. Therefore, characterization of radical ions is usually limited to X-ray structural analysis and UV-vis-NIR and NMR spectroscopic analysis (for singlet dications).

**4.3. Spectral Measurements.** Optical spectra were acquired on a UV-vis spectrometer (200–1100 nm) and UV-vis-NIR spectrophotometer (200–3000 nm), by use of a capped quartz cuvette with side arms. Low-temperature measurements were performed by cooling to the corresponding temperature of solution in Dewar under inert atmosphere and rapid scanning of the cold sample under survey scan

control mode (baseline correction was measured similarly with pure solvent). Variable-temperature  $^1\text{H}$  NMR data for  $\mathbf{1}(\text{Bz})^{2+}\cdot 2[\text{SbF}_6]^-$  were recorded in the solvent system of 2:1 mixture by volume of  $\text{CD}_3\text{OD}/\text{CD}_3\text{CN}$ . At  $-50^\circ\text{C}$ ,  $^1\text{H}$  NMR aromatic H shifts ( $\delta$ ) uns 7.25 (m), 6.20 (s), 5.97 (s), 5.76 (s), 5.18 (s), 4.66 (s), 3.8 (m), and 3.05 (s). None of the conformations present were clearly observed, due to low solubility of the diradical dication at lower temperatures and to broad signals. So we cannot estimate the amounts of syn, anti, and uns conformations that might be present.

## ■ ASSOCIATED CONTENT

### ■ Supporting Information

Additional text, 11 figures, and 12 tables showing comparison of optical spectra of  $\mathbf{1}(\text{Et})^+$  and  $\mathbf{1}(\text{Bz})^+$  in  $\text{CH}_2\text{Cl}_2$ ; UV-vis and  $^1\text{H}$  and  $^{13}\text{C}$  NMR spectral data on  $\mathbf{1}(\text{Bz})$ ; X-ray structure reports on crystal structures of  $\mathbf{1}(\text{Bz})^{2+}\cdot 2[\text{SbF}_6]^-$  and  $\mathbf{1}(\text{Bz})^{2+}\cdot 2[\text{CB}]^-$  (PDF); CIF files. This material is available free of charge via the Internet at <http://pubs.acs.org>.

## ■ AUTHOR INFORMATION

### Corresponding Author

\*E-mail [almaz.jalilov@gmail.com](mailto:almaz.jalilov@gmail.com)

### Present Address

$^\dagger$ (A.S.J.) Department of Chemistry, Northwestern University, 2145 Sheridan Rd., Evanston, IL 60208-3113.

### Notes

The authors declare no competing financial interest.

## ■ ACKNOWLEDGMENTS

We thank the National Science Foundation for support of this work under GM 0647719. We also thank Professor J. Michl for providing  $\text{Cs}^+\text{CB}^-$  salt, Professor R. Rathore for assistance with reflectance spectral measurements, and Professor J. F. Berry for electrochemical instrumentation.

## ■ REFERENCES

- (1) Roth, H. D. *Tetrahedron* **1986**, *42*, 6097–6100.
- (2) (a) Zard, S. Z. *Radical Reactions in Organic Synthesis*; Oxford University Press: New York, 2003. (b) Schmittel, M.; Burghart, A. *Angew. Chem., Int. Ed.* **1997**, *36*, 2550–2589.
- (3) (a) *Magnetism: Molecules to Materials*; Miller, J. S., Drillon, M., Eds.; Wiley-VCH: Weinheim, Germany, 2002; Vol. I–V. (b) Buchachenko, A. L. *Russ. Chem. Rev.* **1990**, *59*, 307–319. (c) Kahn, O. *Molecular Magnetism*; VCH Publishers, Inc.: New York, 1993. (d) Miller, J. M.; Epstein, A. J. *Angew. Chem., Int. Ed.* **1994**, *33*, 385–415.
- (4) (a) Hicks, R. G. *Stable Radicals: Fundamentals and Applied Aspects of Odd-Electron Compounds*; John Wiley & Sons: Chichester, U.K., 2010; p 3. (b) Lahti, P. M. *Magnetic Properties of Organic Materials*; Marcel Dekker: New York, 1999. (c) Fujita, W.; Awaga, K. *Science* **1999**, *286*, 261–262. (d) Facchetti, A. *Mater. Today* **2007**, *10*, 28–37.
- (5) Ingold, K. U. In *Free Radicals*; Kochi, J. K., Ed.; Wiley: New York, 1973; Vol. 1, p 39.
- (6) (a) Pal, S. K.; Bag, P.; Sarkar, A.; Chi, X.; Itkis, M.; Tham, F.; Donnadiu, B.; Haddon, R. J. *Am. Chem. Soc.* **2010**, *132*, 17258–17264. (b) Lakin, K.; Winter, S. M.; Downie, L. E.; Bao, X.; Tse, J. S.; Desgreniers, S.; Secco, R. A.; Dube, P. A.; Oakley, R. T. *J. Am. Chem. Soc.* **2010**, *132*, 16212–16224. (c) Hicks, R. G. *Nat. Chem.* **2011**, *3*, 189–191. (d) Shuvaev, K. V.; Passmore, J. *Coord. Chem. Rev.* **2013**, *257*, 1067–1091.
- (7) (a) Soos, Z. G.; Klein, D. J. *Molecular Association*, Vol. 1; Foster, R., Ed.; Academic: New York, 1975. (b) Miller, J. S., Ed. *Extended Linear Chain Compounds*, Vols. 2 and 3; Plenum Press: New York, 1983. (c) Goto, K.; Kubo, T.; Yamamoto, K.; Nakasuji, K.; Sato, K.;

Shiomi, D.; Takui, T.; Kubota, M.; Kobayashi, T.; Yakushi, K.; Ouyang, J. *J. Am. Chem. Soc.* **1999**, *121*, 1619–1628.

(8) Small, D.; Zaitsev, V.; Jung, Y.; Rosokha, S. V.; Head-Gordon, M.; Kochi, J. K. *J. Am. Chem. Soc.* **2005**, *127*, 7411–7420.

(9) Michaelis, L.; Granick, S. *J. Am. Chem. Soc.* **1943**, *65*, 1747–1755.

(10) (a) Kimura, K.; Yamada, H.; Tsubomura, H. *J. Chem. Phys.* **1968**, *48*, 440–444. (b) Nakayama, S.; Suzuki, K. *Bull. Chem. Soc. Jpn.* **1973**, *46*, 3694–3698.

(11) de Boer, J. L.; Vos, A. *Acta Cryst. B* **1972**, *28*, 835–848.

(12) (a) Kosower, E. M.; Cotter, J. L. *J. Am. Chem. Soc.* **1964**, *86*, 5524–5527. (b) Kosower, E. M.; Hajdu, J. *J. Am. Chem. Soc.* **1971**, *93*, 2534–2535. (c) Kosower, E. M. *Top. Curr. Chem.* **1983**, *112*, 117–162.

(13) Kimura, K.; Yamada, H.; Tsubomura, H. *J. Chem. Phys.* **1968**, *48*, 440–444.

(14) Nakayama, S.; Suzuki, K. *Bull. Chem. Soc. Jpn.* **1973**, *46*, 3694–3698.

(15) Yamagishi, A. *Bull. Chem. Soc. Jpn.* **1975**, *48*, 2440–2447.

(16) Boyd, R. H.; Phillips, W. D. *J. Chem. Phys.* **1965**, *43*, 2927–2929.

(17) Nuvoa, J. J.; Lafuente, P.; Del Sesto, R. E.; Miller, J. S. *Angew. Chem., Int. Ed.* **2001**, *40*, 2540–2545.

(18) Del Sesto, R. E.; Miller, J. S.; Lafuente, P.; Nuvoa, J. J. *Chem.—Eur. J.* **2002**, *8*, 4894–4908.

(19) Miller, J. S.; Nuvoa, J. J. *Acc. Chem. Res.* **2007**, *40*, 189–196.

(20) Head-Gordon, M.; Jung, Y. *Phys. Chem. Chem. Phys.* **2004**, *6*, 2008–2011.

(21) Mota, F.; Miller, J. S.; Nuvoa, J. J. *J. Am. Chem. Soc.* **2009**, *131*, 7699–7709.

(22) Tian, H.; Kertesz, M. *J. Am. Chem. Soc.* **2010**, *132*, 10648–10649.

(23) Grampp, G.; Landgraf, S.; Rasmussen, K.; Strauss, S. *Spectrochim. Acta A* **2002**, *58*, 1219–1226.

(24) Lu, J.-M.; Rosokha, S. V.; Kochi, J. K. *J. Am. Chem. Soc.* **2003**, *125*, 12161–12171.

(25) Geuder, W.; Hünig, S.; Suchy, A. *Tetrahedron* **1986**, *42*, 1665–1677.

(26) Nelsen, S. F.; Li, G.; Schultz, K. P.; Guzei, I. A.; Tran, H. Q.; Evans, D. A. *J. Am. Chem. Soc.* **2008**, *130*, 11620–11622.

(27) Jalilov, A. S.; Li, G.; Nelsen, S. F.; Guzei, I. A.; Wu, Q. *J. Am. Chem. Soc.* **2010**, *132*, 6176–6184.

(28) Rosspeintner, A.; Griesser, M.; Matsumoto, I.; Teki, Y.; Li, G.; Nelsen, S. F.; Gescheidt, G. *J. Phys. Chem. A* **2010**, *114*, 6487–6495.

(29) Jalilov, A. S.; Nelsen, S. F.; Guzei, I. A.; Wu, Q. *Angew. Chem., Int. Ed.* **2011**, *50*, 6860–6864.

(30) Robin, M. B.; Day, P. *Adv. Inorg. Radiochem.* **1967**, *10*, 247–422.

(31) (a) Telo, J. P.; Moneo, A.; Carvalho, F. N. N.; Nelsen, S. F. *J. Phys. Chem. A* **2011**, *115*, 10738–10743. (b) Barriere, F.; Camire, N.; Geiger, W. E.; Mueller-Westerhoff, U. T.; Sanders, R. *J. Am. Chem. Soc.* **2002**, *124*, 7262–7273.

(32) Evans, D. H. *Chem. Rev.* **2008**, *108*, 2113–2144.

(33) (a) Rosokha, S. V.; Newton, M.; Jalilov, A. S.; Kochi, J. K. *J. Am. Chem. Soc.* **2008**, *130*, 1944–1952. (b) Nelsen, S. F. *Chem.—Eur. J.* **2000**, *6*, 581–588.

(34) (a) Rosokha, S. V.; Kochi, J. K. *J. Am. Chem. Soc.* **2007**, *129*, 3683–3697. (b) Rosokha, S. V.; Kochi, J. K. *Acc. Chem. Res.* **2008**, *41*, 641–653.

(35) Nelsen, S. F.; Weaver, M. N.; Telo, J. P. *J. Am. Chem. Soc.* **2007**, *129*, 7036–7043.

(36) (a) Evans, D. H. *Chem. Rev.* **2008**, *108*, 2113–2144. (b) Adams, C. J.; DaCosta, R. C.; Edge, R.; Evans, D. H.; Hood, M. F. *J. Org. Chem.* **2010**, *75*, 1168–1178.

(37) (a) Korbe, S.; Schreiber, P. J.; Michl, J. *Chem. Rev.* **2006**, *106*, 5208–5249. (b) Douvris, C.; Michl, J. *Chem. Rev.* **2013**, *113* (10), PR179–PR233.

(38) Zalibera, M.; Jalilov, A. S.; Stroll, S.; Guzei, I. A.; Gescheidt, G.; Nelsen, S. F. *J. Phys. Chem. A* **2013**, *117*, 1439–1448.

(39) Punyain, K.; Kelterer, A.-M.; Grampp, G. *Spectrochim. Acta A* **2011**, *83*, 368–378.



(40) Hayashi, Y.; Rohde, J. J.; Corey, E. J. *J. Am. Chem. Soc.* **1996**, *118*, 5502–5503.